Article

Trigger Factor Assisted Folding of Green Fluorescent Protein
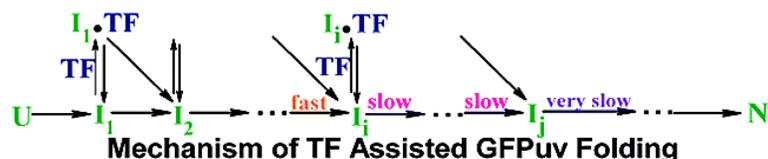
Jiang-Bi Xie, and Jun-Mei Zhou

Equilibrium Unfolding and Dynamic Refolding of GFPuv

Mechanism of TF Assisted GFPuv Folding

More About This Article

Additional resources and features associated with this article are available within the HTML version:

- Supporting Information
- Access to high resolution figures
- Links to articles and content related to this article
- Copyright permission to reproduce figures and/or text from this article

View the Full Text HTML

ACS Publications
High quality. High impact.

Trigger Factor Assisted Folding of Green Fluorescent Protein[†]

Jiang-Bi Xie and Jun-Mei Zhou*

National Laboratory of Biomacromolecules, Institute of Biophysics, Chinese Academy of Sciences, 15 Datun Road, Beijing 100101, China

Received June 15, 2007; Revised Manuscript Received September 18, 2007

ABSTRACT: Guanidine induced equilibrium and kinetic folding of a variant of green fluorescent protein (F99S/M153T/V163A, GFPuv) was studied. Using manual mixing and stopped-flow techniques, we combined different probes, including tryptophan fluorescence, chromophore fluorescence and reactivity with DTNB, to trace the spontaneous and TF-assisted folding of guanidine denatured GFPuv. We found that both unfolding and refolding of GFPuv occurred in a stepwise manner and a stable intermediate was populated under equilibrium conditions. The thermodynamic parameters obtained show that the intermediate state of GFPuv is quite compact compared to the denatured state and most of the green fluorescence is retained in this state. By studying GFPuv folding assisted by TF and a number of TF mutants, we found that wild-type TF catalyzes proline isomerization and accelerates the folding rate at low TF concentrations, but retards GFPuv folding and decelerates the folding rate at high TF concentrations. This reflects the two activities of TF, as an enzyme and as a chaperone. A general mechanism of TF assisted protein folding is discussed.

Green fluorescent protein (GFP[1]), originally isolated from the jellyfish *Aequorea victoria*, is a single domain globular protein of 238 amino acids, which autocatalytically generates a covalently attached chromophore when correctly folded and therefore fluoresces without external cofactors. GFP is remarkable for its structural stability and high fluorescence quantum yield. GFP and its analogues have been used extensively in biological and medical research as a marker of gene expression and protein localization (*1*); as an efficient tracer in physiological investigations (*2*); as an indicator of protein−protein interactions (*3*) or a reporter of the folding of fusion proteins (*4, 5*); and even as a biosensor (*6*). GFP is a typical β-barrel protein. Its mutant, GFPuv or c3−GFP (F99S/M153T/V163A), is cylindrical in shape and comprises 11 β-strands with one α-helix inside and short helical segments on the ends of the cylinder (Figure 1). The cylinder has a diameter of about 30 Å and a length of about 40 Å. The highly protected chromophore (Ser65/Tyr66/Gly67) is located on the central helix within a couple of angstroms of the geometric center of the cylinder (*7*). Although 42-fold more fluorescent than wild-type GFP, GFPuv has the same spectral characteristics, topology and overall structure as wild type, as well as similar folding and hydrogen-exchange behavior (*8*).
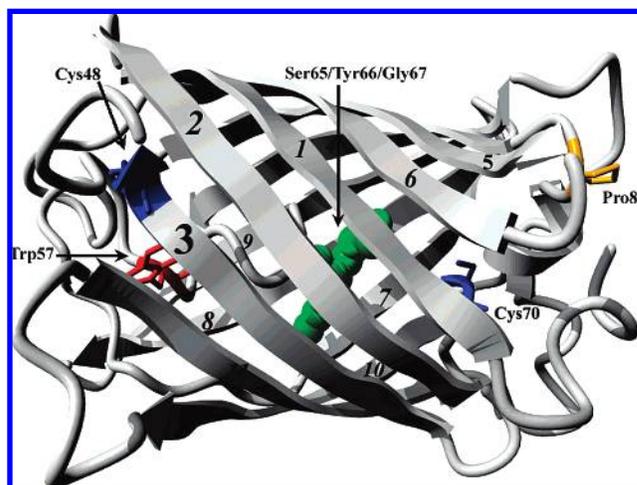

FIGURE 1: Ribbon diagram of the backbone structure of the GFP mutant, GFPuv (Protein Data Bank code 1b9c), with the chromophore (Ser65/Tyr66/Gly67) and the side chains of other residues: Cys48, Trp57, Cys70 and Pro89 (*cis*-configuration), displayed in ball and stick style. The β-strands are numbered from the N to the C terminus. The figure was created with the program YASARA (http://www.yasara.org); also using YASARA, the secondary structure content was analyzed giving 2.7% α-helix, 54.0% β-sheet, 22.8% turn and 20.5% coil.

The folding efficiency of GFP is known to limit its use in a number of applications. To date, many studies have already been carried out on the folding and unfolding kinetics of GFP (*7−10*). For example, the Kuwajima group has investigated the folding of GFPuv in detail by acid denaturation (*11, 12*); and the Jackson group found that GFP significantly populates an intermediate state under equilibrium conditions during chemical denaturation (*13*). Recently, a superfolder GFP has been engineered and characterized (*14*). The effect of a number of molecular chaperones on the folding of GFP has also been studied, such as trigger factor (TF) from

[1] Abbreviations: GFP, green fluorescent protein; GFPuv, the GFP mutant, F99S/M153T/V163A; TF, trigger factor; PPIase, peptidyl-prolyl *cis/trans* isomerase; Tris, tri(hydroxymethyl)aminomethane; DNase I, deoxyribonuclease I; GuHCl, guanidine hydrochloride; DTNB, 5,5′-dithio-bis(2-nitrobenzoic acid); EG, ethylene glycol; BSA, bovine serum albumin (fraction V); FRET, fluorecence resonance energy transfer.

Thermus thermophilus (*15*), Hsp70 and Hsp100 chaperones (*16*) and the chaperonins (*17*). Here, we describe investigation of the folding of guanidine-denatured GFPuv in the presence and absence of *Escherichia coli* TF.

TF, a 48 kDa protein with a modular structure, is the first chaperone that nascent polypeptides encounter in *Escherichia coli* (*18*). It forms a protective shield for nascent polypeptides at the ribosome exit tunnel and assists the folding of most newly synthesized polypeptide chains (*19*, *20*). TF is also a peptidyl-prolyl *cis/trans* isomerase (PPIase) (*18*, *21*), and the catalytic center of enzyme activity lies in the M domain, which has structural homology to FK506-binding proteins (*22*, *23*) and forms the head domain of the TF molecule (*24*). However, the PPIase activity of TF is dispensable to its chaperone activity (*25−27*). It has been concluded that both the C-terminal domain and part of the N-terminal domain of TF are essential for its chaperone activity (*27−29*) and the C domain, together with a segment of the N domain, forms the "back" and "arms" of the TF structure, which orients its hydrophobic inner surface toward emerging nascent polypeptides (*24*). Most ribosomes exist in a 1:1 complex with TF, consistent with the role of TF in cotranslational protein folding (*24*, *30*). However, TF is present in a 2−3-fold molar excess over ribosomes in the cell, with the majority of free TF present as a dimer (*31*), and the dynamic monomer−dimer equilibrium of TF contributes to the regulation of the accessibility of its chaperone sites (*32*, *33*). TF is an efficient molecular chaperone in the catalysis of protein folding reactions which are rate-limited by isomerization of prolyl bonds (*34*). *In vitro* studies of TF-assisted GAPDH (*35*), bovine carbonic anhydrase II (*36*) and lysozyme (*37*) folding have revealed that TF is not only a prolyl isomerase but also a chaperone. TF binds preferentially to protein substrates with loose tertiary structure (*35*), which is consistent with the ability of TF to bind to newly synthesized nascent chains which are at an early stage in the folding process *in vivo*.

Here, we combined different probes, including tryptophan fluorescence, chromophore fluorescence and the reactivity with DTNB, to trace the spontaneous and TF-assisted folding of guanidine denatured GFPuv. The results revealed that both the unfolding and refolding of GFPuv are gradual processes and a stable intermediate is populated under equilibrium conditions. The folding of GFPuv, assisted by TF and a number of TF mutants, demonstrates clearly the involvement of the two functions of TF, as an enzyme and as a chaperone.

MATERIALS AND METHODS

Reagents. GuHCl (ultrapure) and Tris were from Fluka. L-(+)-Arabinose, DNase I, DTT, the sulfhydryl reagent DTNB and BSA were all from Sigma. Other chemicals were local products of analytical grade. The concentration of GuHCl solutions was determined using an Abbe refractometer (Atago, Japan) and calculated according to the formula

$$[GuHCl] = 57.147(\Delta N) + 38.68(\Delta N^2) - 91.60(\Delta N^3)$$

where ΔN is the refractive index of the solution measured at 589 nm and 20 °C (*38*).

Methods. All equilibrium spectral measurements and kinetic unfolding and refolding measurements of GFPuv were performed at 25 °C. Concentrations of proteins were

determined by UV absorption using extinction coefficients at 280 nm, as follows: GFPuv (2.00×10^4 M^{-1} cm^{-1}), TF (1.59×10^4 M^{-1} cm^{-1}) and TF mutants, F233Y-TF (1.72×10^4 M^{-1} cm^{-1}), F233Y C389 (1.72×10^4 M^{-1} cm^{-1}), NM (1.34×10^4 M^{-1} cm^{-1}), MC (1.00×10^4 M^{-1} cm^{-1}), NC (0.90×10^4 M^{-1} cm^{-1}), calculated using the procedure of Gill and von Hippel (*39*).

(1) Protein Expression and Purification. GFPuv was expressed in *E. coli* HB101 transformed with the pGLO plasmid (BioRad) and cultured at ≤30 °C. GFPuv overproduction was induced by L-(+)-arabinose addition. The bacterial lysate in buffer A (10 mM Tris-HCl, pH 8.0, 1 mM EDTA) was centrifuged at 20000*g* for 1 h. The green fluorescent supernatant was collected and treated with DNase I for about 10 min. Protein purification was carried out as follows: (a) Differential ammonium sulfate precipitation. We mixed one volume ratio of binding buffer (buffer B (4.0 M (NH$_4$)$_2$SO$_4$) in buffer A) gently and slowly into the translucent solution at room temperature. The turbid mixture was centrifuged and the supernatant was collected. (b) Hydrophobic interaction chromatography. The sample was loaded on a Butyl-sepharose 4 Fast Flow column (Amersham Biosciences) and washed sequentially with equilibrium buffer (buffer C (2.0 M (NH$_4$)$_2$SO$_4$) in buffer A) and wash buffer (buffer D (1.3 M (NH$_4$)$_2$SO$_4$) in buffer A). The above operations were carried out at room temperature. The green fluorescent fractions were then eluted using buffer A and concentrated by ultrafilter centrifugation at 4 °C. The concentrated sample was purified further by (c) gel filtration using a Sephadex G-75 column (Amersham Biosciences) and (d) ion-exchange chromatography using DEAE-Sepharose Fast Flow resin (Amersham Biosciences) with a gradient elution of 0−0.2 M NaCl in buffer A. Finally, the GFPuv peak with visible green fluorescence was collected, concentrated and stored at −80 °C.

Plasmid pQE60 containing the wild-type *tig* gene that encodes *E. coli* TF was donated by Professor G. Fischer. TF and domain deletion mutants NM, MC, NC were constructed with a 6×His tag on their N-terminus and were purified by elution with imidazole from a chelating Sepharose Fast Flow Ni-column (Amersham Biosciences); while other mutants F233Y-TF (*25*) and F233Y C389 (*40*) were purified according to the published protocols.

The purity of all proteins was confirmed by SDS−PAGE and the ratio of the absorbance at 397 nm to that at 280 nm for GFPuv was higher than 1.1, which is an indicator of the purity of GFP (*41*).

(2) Monitoring of the Dynamic Unfolding of GFPuv by the Ellman Reaction. The determination of thiol groups was carried out using DTNB as described by Ellman (*42*) with a UV-4802 spectrophotometer (UNIC, Shanghai) at 25 °C. To make a stock solution of Ellman's reagent, DTNB was dissolved in 50 mM Tris buffer pH 7.5 to give a final concentration of 10 mM and the pH was adjusted again to pH 7.5 by adding NaAc or NaHCO$_3$; the solution was stored at 4 °C. In order to measure the number of reactive −SH groups, both the reference and sample cells contained 0.1 mM DTNB in 50 mM Tris buffer pH 7.5 with 10 μM native or 6 M guanidine denatured GFPuv added to the sample cell. The number of reactive −SH groups was evaluated using a molar absorbance coefficient of 13,600 M^{-1} cm^{-1} at 412 nm. In order to follow the time course of the change in

exposure of −SH groups during GFPuv unfolding, an aliquot of 10 μM GFPuv was unfolded in 6 M guanidine and aliquots were removed at different time intervals, added to the reaction system containing 0.1 mM DTNB and allowed to react for 30 s. The absorbance of the same solution without GFPuv was recorded at 412 nm as the reference. The change of absorbance at 412 nm during GFPuv unfolding in the absence of DTNB was also monitored.

(3) Fluorescence Measurements. All experiments were carried out in 50 mM Tris-HCl pH 7.5 containing 100 mM NaCl, 1 mM EDTA and 5 mM (or 1 mM) DTT with or without GuHCl, unless otherwise stated. Since the unfolded states of GFPuv are denaturant concentration and incubation time dependent, the refolding experiments were started from a stock solution of GFPuv denatured in 6.0 M GuHCl for 16 h.

GuHCl-induced GFPuv (1 μM) equilibrium unfolding experiments were performed as described (*38*). After 24 h incubation, the emission intensities of the protein in buffer containing different concentrations of GuHCl were measured at different excitation wavelengths.

For those kinetic unfolding and refolding measurements which were performed after 5 s manual mixing on a HITACHI F-4500 fluorescence spectrophotometer (Hitachi High-Technologies Corporation, Tokyo, Japan), the slit widths were set at 2.5 nm for both excitation and emission unless otherwise stated. All the manual mixing renaturation reactions were initiated upon 100-fold dilution from 6.0 M GuHCl into renaturation buffer with or without additives, such as BSA, TF, TF mutants, GuHCl or ethylene glycol (EG). For renaturation systems with different pH values, 50 mM Tris, phosphate or sodium acetate buffer was prepared to give final pH values of 7.5, pH 7.0−6.0 or pH 5.6, respectively.

For those rapid kinetic folding measurements which were performed on a π^*-180 PiStar stopped-flow apparatus (Applied Photophysics, Surrey, U.K.), both of the slit widths were set at 5 nm and the dead time of the standard 20 μL optical cell is 1 ms. Unfolding reactions were initiated by mixing the native protein with 6.6 M GuHCl in a volume ratio of 1:10, and the final concentration of GuHCl was 6.0 M. For the refolding reactions, in order to obtain a high degree of dilution (about 52-fold) we used the instrument in sequential multimixing mode (1:25 followed by 1:1 dilutions with a delay period of 0.01 s). This was done in order to minimize the effect of residual GuHCl on GFPuv refolding; the residual GuHCl concentration was about 0.12 M.

(4) Data Analysis. (a) Analysis of Equilibrium Data. All fluorescence data were fitted to a two or three-state model as described (*38*, *43* and references therein). When two transitions were observed, the curve was analyzed using a three-state model, N ↔ I ↔ U, where N, I, and U are native, intermediate and unfolded states, respectively, and, the fractions, *f*, of the respective species are given as $f_N + f_I + f_U = 1$. Since GFPuv is monomeric under the experimental concentrations used here, the simplest unfolding model was used.

(b) Kinetic Analysis. The unfolding and refolding kinetic data were fitted using the program SigmaPlot2000 according to the following equations (nonlinear regression):

$$A(t) = A_0 + \sum \Delta A_i \exp(-k_i t) \qquad (1)$$

for unfolding, where $A(t)$ is the fluorescence intensity at time t and A_0 is the initial value, and

$$A(t) = A_0 + \sum \Delta A_i (1 - \exp(-k_i t)) \qquad (2)$$

for refolding, where $A(t)$ and A_0 are the fluorescence intensities at time t and the starting time, respectively; and ΔA_i and k_i are the amplitude and the apparent rate constant of the *i*th phase, respectively.

RESULTS

GFPuv Unfolding Is a Gradual Process and an Intermediate Is Maximally Populated around 3.5 M GuHCl. Guanidine induced unfolding of GFPuv was monitored by changes in intrinsic fluorescence, chromophore fluorescence and the exposure of cysteine residues. GFPuv shows maximum fluorescence emission at 508 nm when excited at either 397 or 280 nm (Figure 2a).

Figure 2b shows the comparison of equilibrium unfolding curves monitored by different fluorescence probes. The transition curves monitored by the three different probes clearly do not coincide. The Trp fluorescence was observed to decrease at lower guanidine concentration than the chromophore fluorescence: after equilibration for 24 h in 2.0 M GuHCl, Trp57 is significantly exposed, while the microenvironment of the chromophore (Ser65/Tyr66/Gly67) is apparently unaffected. Only when the GuHCl concentration was higher than 3.0 M, where Trp57 has already become totally exposed to the solvent, was there a conspicuous drop in the chromophore fluorescence. There is a single Trp residue (Trp57) and eleven Tyr residues distributed over the GFPuv molecule; one Tyr residue is an integral part of chromophore. When following the changes in chromophore fluorescence after excitation at 280 nm, fluorescence resonance energy transfer (FRET) between Trp57 and the Ser65/Tyr66/Gly67 chromophore was observed. The parameters obtained by fitting the data to a two- or three-state model are shown in Table 1. The changes in chromophore or tryptophan fluorescence, when monitored independently, show a highly co-operative two-state transition. However, combined monitoring of the two probes by the observed FRET signal allows fitting to a three-state model and shows that, under equilibrium conditions, an intermediate (I) is maximally populated at around 3.5 M GuHCl (Figure 2b). The intermediate is energetically closer to the native state than to the fully denatured state (Table 1) and retains more than 90% of the specific green fluorescence (Figure 2b). In this intermediate state, the microenvironment around the chromophore is disturbed only partially although Trp57 is already extensively exposed. This conclusion can be corroborated by the results of the Kuwajima group showing that the unfolding transition for GFPuv measured by far-UV CD coincides with the one measured by green fluorescence (*8*), which means that the change in emitted green fluorescence directly reflects the change in secondary structure of GFPuv. Recently, a similar intermediate state, which is compact and stable with respect to the unfolded state, was identified by the Jackson group who monitored changes in structure by green fluorescence, tyrosine fluorescence and far-UV circular
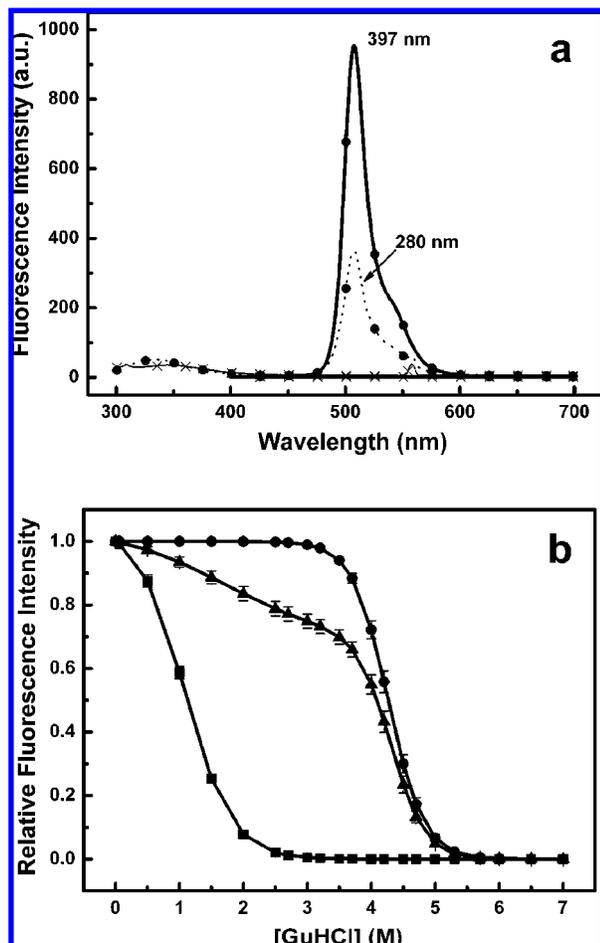
FIGURE 2: (a) Emission spectra of GFPuv in the native state (●) and the 6.0 M GuHCl unfolded state (×) after exitation at 397 nm (—) and 280 nm (⋯), in 50 mM Tris-HCl buffer, pH 7.5, containing 100 mM NaCl, 1 mM EDTA and 5 mM DTT. (b) GuHCl induced equilibrium unfolding of GFPuv measured by chromophore fluorescence at 508 nm when excited at 280 nm (▲) or 397 nm (●), and by tryptophan fluorescence at 335 nm (■) when excited at 280 nm. The error bars represent the standard error of the mean of 3 repeated measurements. Thermodynamic parameters obtained by fitting the data to a two- or three-state unfolding model are displayed in Table 1.

dichroism (*13*). Taken together, this indicates that the intermediate is close in stability to the native state and maintains nativelike secondary structure, thus it may best be described as a native-like intermediate.

We used the two fluorescent probes to further monitor changes in the microenvironments of Trp57 and the chromophore during kinetic unfolding of GFPuv (Figure 3). When GFPuv was exposed to 6.0 M GuHCl, the fluorescence intensity of Trp57 decreased rapidly and the process could be fitted to three kinetic phases with rate constants of 14.85 ± 0.43 s^{-1}, 3.78 ± 0.19 s^{-1} and 0.46 ± 0.03 s^{-1} (Figure 3a). However, the change in chromophore fluorescence was extremely slow, with an unfolding rate constant of 5.24×10^{-4} s^{-1} (Figure 3c). The very slow unfolding rate of GFPuv even at high chemical denaturant concentrations suggests that there is a high kinetic energy barrier for unfolding (Figure 3c). However, 6.0 M GuHCl is sufficient to completely denature GFPuv (Figure 2b) and the free energy of unfolding (45.2 kJ/mol) is not exceptionally high for a protein of this size (Table 1).

There are two cysteine residues in GFPuv, Cys48 and Cys70, which do not form a disulfide bond and are located nearly at opposite ends of the cylinder (Figure 1). The two Cys residues lie between β-strands 3 and 4, with Cys48 located within the β-sheet and Cys70 in a turn. Cys48 may be partially solvent accessible while Cys70 is buried within the core of the protein. We found here that native GFPuv reacts with DTNB with a stoichiometry of about 0.5 DTNB per GFPuv molecule, which can be ascribed to the contribution of Cys48; while fully denatured GFPuv reacts with about 2.0 DTNB molecules per GFPuv molecule, consistent with full exposure of both cysteine residues on unfolding of GFPuv. The rate of unfolding of GFPuv in 6.0 M GuHCl obtained by monitoring the exposure of cysteine residues $((3.8 \pm 0.2) \times 10^{-4}$ s$^{-1})$ (Figure 4) is around 3-fold slower than the rate constant $((10.8 \pm 0.4) \times 10^{-4}$ s$^{-1})$ obtained by monitoring chromophore fluorescence at 10 μM GFPuv concentration. This suggests that the β-barrel structure is at least partly maintained after the chromophore fluorescence has already been quenched.

We therefore conclude that the unfolding of GFPuv is a stepwise process in which exposure of Trp57 occurs first, followed by exposure of the chromophore, and then finally the whole β-barrel backbone unfolds.

The Refolding of GFPuv Involves Rapid Burial of the Tryptophan Residue Followed by Slow Acquisition and Even Slower Adjustment of the Microenvironment around the Chromophore. The changes in tryptophan fluorescence and chromophore fluorescence during refolding of GFPuv were also compared (Figure 3). When 6.0 M GuHCl denatured GFPuv was diluted with buffer to give a final GuHCl concentration of 0.12 M by sequential multimixing in a stopped-flow instrument (see methods), a burst phase increase in tryptophan fluorescence was observed within the dead time of the stopped-flow apparatus, and this was followed by a biphasic fast increase in the fluorescence with rate constants of 2.04 s^{-1} and 0.13 s^{-1} (Figure 3b). However, the increase in chromophore fluorescence during refolding is relatively slow (Figure 3c). The refolding curve when monitoring chromophore fluorescence was biphasic, and fitting to a double exponential yielded the rate constants $k_1 = 5.29 \times 10^{-2}$ s^{-1} and $k_2 = 0.91 \times 10^{-2}$ s^{-1}, suggesting that the microenvironment around the chromophore is formed and then undergoes further adjustment. After about 100 s, we could observe a gradual quenching of the tryptophan fluorescence as the chromophore fluorescence was regained, suggesting a slow adjustment of the specific tertiary structure in the vicinity of the chromophore (Figure 3d). This slow adjustment could also be related to prolyl isomerization within the GFPuv molecule (*11*). Although in both cases a burst phase is observed, the change of tryptophan fluorescence of GFPuv refolding after guanidine denaturation (Figure 3b) is quite different from that after acid denaturation observed by Kuwajima group (*11*), in which the tryptophan fluorescence increased first and then decreased accompanying GFPuv refolding. The difference may come from the different denaturation methods used since fluorescence is an extremely sensitive technique and the tryptophan fluorescence of a protein depends strongly on the degree of tryptophan exposure and on the solvent conditions.

We further investigated the effect of residual guanidine concentration on GFPuv refolding. The refolding rate

Table 1: Thermodynamic Parameters for GuHCl Denaturation of GFPuv[a]

method	ΔG_{IN} (kJ mol^{-1})	ΔG_{UI} (kJ mol^{-1})	ΔG_{UN} (kJ mol^{-1})	m_{IN} (kJ mol^{-1} M^{-1})	m_{UI} (kJ mol^{-1} M^{-1})	y_I (%)	[D]$_{1/2,IN}$ (M)	[D]$_{1/2,UI}$ (M)
Trp fluorescence[b]	-7.4 ± 1.2			6.9 ± 1.0			1.09	
chromophore fluorescence								
excited at 397 nm[b]		38.0 ± 1.1			8.9 ± 0.6			4.27
excited at 280 nm	-5.0 ± 1.8	-40.2 ± 3.2	-45.2 ± 4.3	3.0 ± 0.5	9.3 ± 1.0	70	1.70	4.31

[a] ΔG is the free energy of unfolding extrapolated to zero denaturant concentration, m is the denaturant dependence, and [D]$_{1/2}$ is the denaturant midpoint of the transition. N, I and U indicate native, intermediate and fully unfolded states, respectively, and y_I is the normalized fluorescence value of the intermediate. For the three-state unfolding model, $\Delta G_{IN} + \Delta G_{UI} = \Delta G_{UN}$. [b] Fitted to a two-state model, and judged to correspond to either ΔG_{IN} or ΔG_{UI}, as shown.

constant monitored by chromophore fluorescence was observed to decrease with increasing residual GuHCl concentration (Table 2) until, eventually, the refolding of GFPuv changed from biphasic to monophasic, although there was almost no change in the total amplitude when the GuHCl concentration was not higher than 0.25 M (data not shown). This is consistent with the previously reported results that the apparent rate constants are GuHCl concentration dependent and the fluorescence recoveries of GFPuv refolding are GuHCl concentration independent when the GuHCl concentration is not higher than 0.25 M (8).

Low Concentrations of Trigger Factor Accelerate Folding of GFPuv. TF assisted GFPuv refolding was investigated in detail. As shown in Figure 5a and Table 2, the refolding of GFPuv in buffer containing 0.18 M GuHCl monitored by chromophore fluorescence is biphasic, with rate constants of $k_1 = (3.57 \pm 0.07) \times 10^{-2}$ s^{-1} and $k_2 = (0.71 \pm 0.10) \times 10^{-2}$ s^{-1}. These two processes are suggested to correlate with rapid recovery of the chromophore microenvironment followed by a further structural adjustment. There are 10 proline residues in GFPuv, one of which, Pro89, is in a *cis*-conformation in the native structure (Figure 1). During GFPuv refolding in the presence of TF, both k_1 and k_2 increased with increasing TF concentration for TF concentrations up to 0.4 μM (Figure 5b, inset). However, at the same low concentrations, the presence of BSA or F233Y-TF (a mutant of TF in which the PPIase activity has been impaired by mutation) showed no effect on the refolding rate constants (Table 3). (It should be noted that, to reduce the possible effect of residual guanidine concentration on the function of TF or TF mutants, the data in Table 3 was obtained in a refolding system in which the residual guanidine concentration was 0.06 M.) We also tested the effects on GFPuv refolding of other TF variants, NC, NM and MC, in which, respectively, the entire M, C or N domain of TF has been deleted. The results showed that the refolding of GFPuv was not affected by low concentrations of those TF variants (Table 3). Two of the truncated variants, NM and MC, show PPIase activity toward small peptides, but their reduced substrate binding ability significantly reduces their efficacy toward protein substrates (44). These results suggest that both the fast and slow phases of GFPuv folding are related to proline isomerization. Low concentrations of wild-type TF can catalyze proline isomerization during refolding, and so the refolding rate is increased.

High Concentrations of Trigger Factor Retard Folding of GFPuv. In contrast to low concentrations of TF, the refolding of GFPuv in the presence of high concentrations of TF was clearly retarded and the rate constants of refolding decreased with increasing TF concentration (Figures 5a and

5b). When the refolding of GFPuv was measured in the presence of 10 μM TF, refolding became monophasic and the rate constant decreased to $(1.00 \pm 0.01) \times 10^{-2}$ s^{-1} (Figures 5a and 5b; Table 2). As a control, BSA (10 μM or 50 μM) had no detectable effect on the rates of GFPuv refolding (Figure 5b), suggesting a specific interaction between TF and GFPuv folding intermediates.

F233Y-TF shows about the same ability in retarding GFPuv refolding as wild-type TF at the high concentration even though it exhibits no PPIase activity toward GFPuv at the low concentration (Table 3), suggesting once again that the PPIase activity of TF is dispensable to its chaperone activity (25−27). A number of investigations have shown that the NC-domain segment of TF alone is sufficient for function as a molecular chaperone *in vivo* (27) and *in vitro* (28). However, the efficiency of NC assisted GAPDH refolding is much lower than that of the full length TF, so that a 10-fold-higher concentration of NC is required to prevent GAPDH aggregation to the same extent as full length TF (28). This can explain why in the presence of high concentrations of NC only mild deceleration of GFPuv refolding was observed in our case (Table 3). High concentrations of the NM or MC fragments show almost no effect on the GFPuv refolding (Table 3), which is consistent with the conclusion of Kramer and co-workers that the full chaperone activity of TF cannot be restored by single domain or domain combinations but needs the coordinated assembly within the entire TF molecule (28). In conclusion, the above results obtained using TF mutants suggest that TF function may depend on the structure of the target protein and that cooperation of the three domains of TF is required to assist GFPuv refolding.

Effect of pH and Solution Hydrophobicity on TF Assisted Refolding of GFPuv. As shown in Figure 6a, at pH values between 6.6 and 7.5, GFPuv refolding showed two phases and the rate constants did not show any obvious pH dependence; while in the presence of 10 μM TF, GFPuv refolding became monophasic and the rate constant also showed little pH dependence over this range. However, at pH values between 5.6 and 6.6, refolding of GFPuv in the presence or absence of TF was monophasic and the rate constants increased with increasing pH. The isoelectric points of GFPuv and TF are predicted to be 5.64 and 4.92, respectively (DNASIS v2.5), and so we did not investigate the refolding at pH lower than 5.6.

Ethylene glycol (EG) is a solvent that can change the hydrophobicity of the solution. When monitoring the chromophore fluorescence of GFPuv, the refolding rate constants, k_1 and k_2, did not show any obvious change with increasing EG concentrations up to 20% at pH 7.5 (Figure 6b). In the
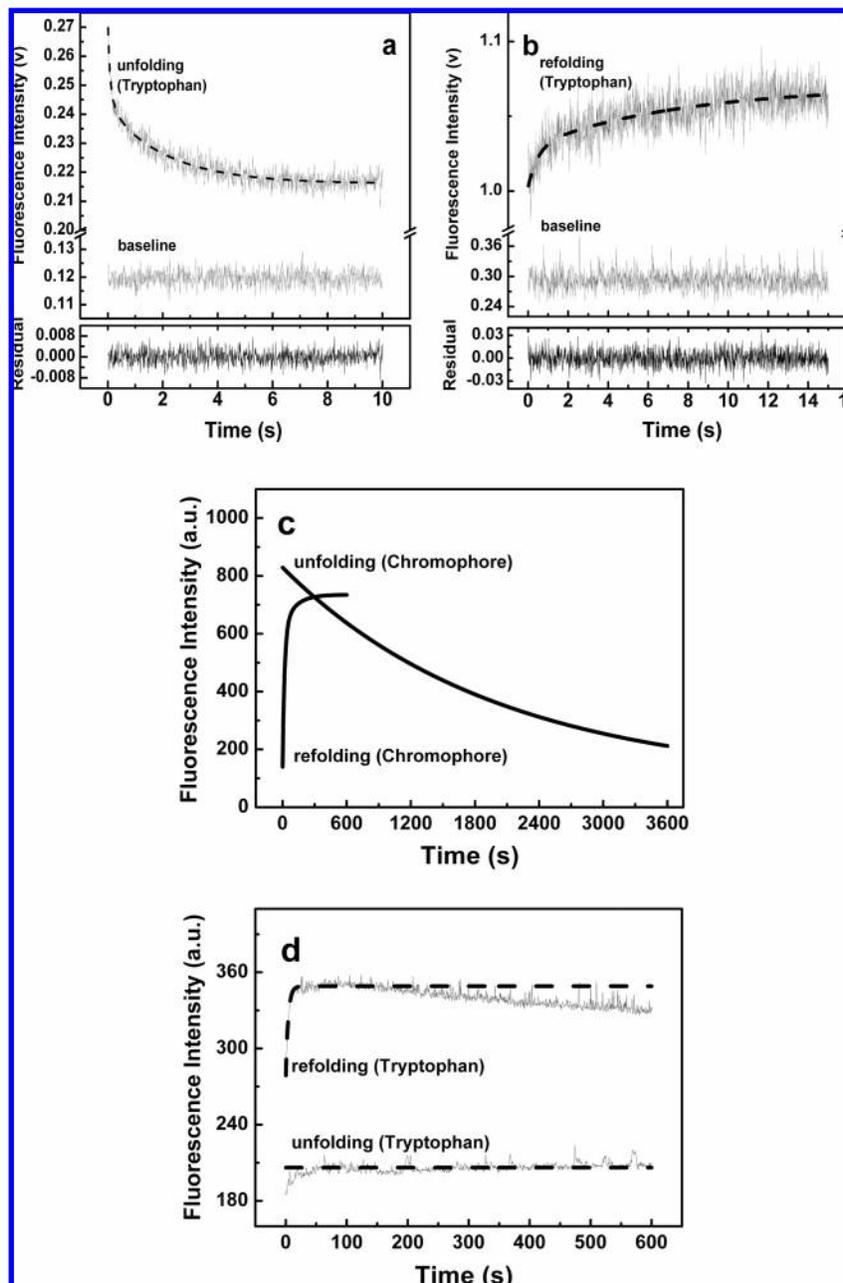
FIGURE 3: Kinetic unfolding (a) and refolding (b) of GFPuv monitored by tryptophan fluorescence using a stopped-flow instrument, with emission at 335 nm and excitation at 293 nm and both slits of 5 nm. The reactions were performed by a jump of GuHCl concentration from 0 to 6.0 M for unfolding and from 6.0 to 0.12 M for refolding. Baselines of the mixing with Tris buffer of the corresponding concentration GuHCl were also plotted in the same frame. Plots of the residuals of the fits are shown in the lower panel. Kinetic folding of GFPuv monitored by chromophore fluorescence (c) and tryptophan fluorescence (d) using manual mixing technique, with emission at 508 nm and excitation at 397 nm and both slits of 2.5 nm for the monitoring of chromophore fluorescence, or with emission at 335 nm and excitation at 293 nm and slits of 10 and 5 nm, respectively, for monitoring tryptophan fluorescence. The reactions were performed by a jump of GuHCl concentration from 0 to 6.0 M for unfolding and from 6.0 to 0.06 M for refolding for both probes. The GFPuv concentration was 1 μM throughout.

presence of 6 μM TF but without EG, the refolding of GFPuv was retarded and became monophasic (Figure 6b); however, with increasing EG concentration, the refolding of GFPuv in the presence of 6 μM TF became biphasic once again and both phases were accelerated, suggesting that hydrophobic interactions provide the major force for interactions between TF and folding intermediates of GFPuv. Changing the hydrophobicity of the solvent perturbs the binding and release of target molecules by TF and so affects the refolding rate constants.

Like most other GFP variants (*45, 46*), the effect of pH on GFPuv can be detected by an intensity change in the chromophore fluorescence, although the positions of the peaks in its chromophore fluorescence spectra are not shifted; and for GFPuv, the highest fluorescence intensity can be obtained at about pH 7.5 (data not shown). This is consistent with a change in the protonation state of the chromophore phenolate (*46*). This then explains why the refolding rates of GFPuv are pH dependent below pH 6.6 (Figure 6a). However, in the presence of high concentrations of TF, the
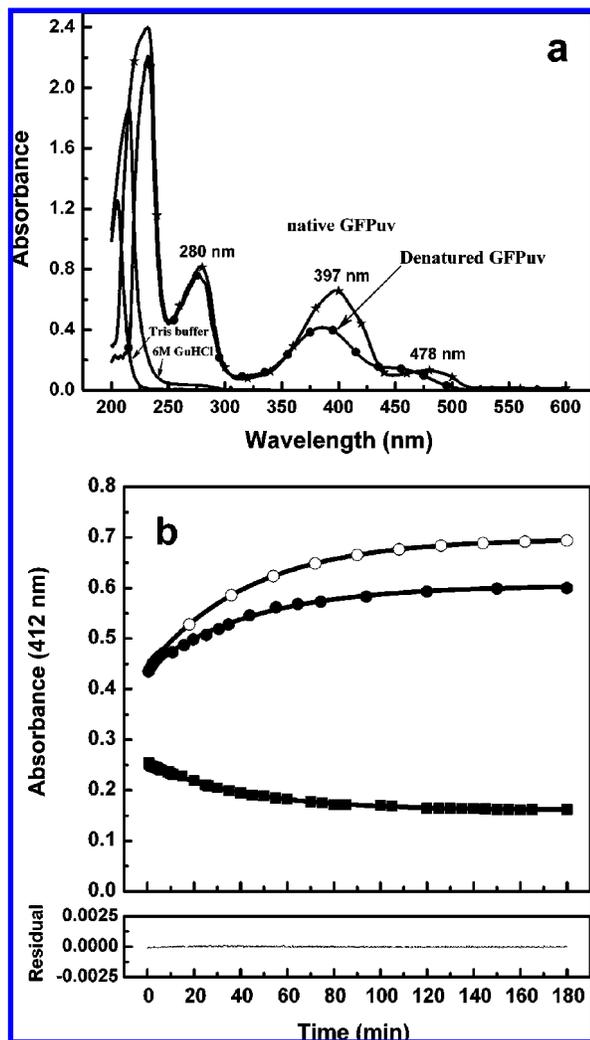
FIGURE 4: Unfolding of GFPuv monitored by the Ellman reaction at 412 nm. (a) Absorption spectra of native (★) and 6.0 M GuHCl denatured (●) GFPuv in Tris buffer, pH 7.5. The absorption of Tris buffer with and without 6.0 M GuHCl is negligible over the range 250−600 nm. The GFPuv was denatured for 33 h in 6.0 M GuHCl. (b) Time courses of GFPuv unfolding in 6.0 M GuHCl followed by Ellman reaction at 412 nm. The protein concentration was 10 μM. The absorbance change of GFPuv during unfolding was measured in the presence of 100 μM DTNB (●). The change of absorbance of GFPuv when unfolding in the absence of DTNB (■) was measured as a control, to eliminate the effect of change not induced by the DTNB-dependent reaction. The actual time course of cysteine exposure (○), from which the non-DTNB-dependent change of absorbance had already been subtracted, was fitted to a single-exponential equation giving a rate constant of $(3.8 \pm 0.2) \times 10^{-4}$ s^{-1}. The plot of the residual between the actual time course and the result obtained by fitting is shown in the lower panel.

combined effects of pH and solvent hydrophobicity on the refolding rates of GFPuv can also be explained by a competition between binding and release of folding intermediates by TF.

DISCUSSION

GFP is a molecule with properties that are quite distinct from most other small single domain proteins (*47*). Both its unfolding and refolding are slow and quite complex (*8*, *11*, *12*). The slowest observable phase in refolding of GFPuv occurs with a half-life of around 64 s at a GuHCl concentra-

Table 2: The Effect of Residual GuHCl on the Apparent Rate Constants of GFPuv Refolding Measured by Chromophore Fluorescence in the Absence and in the Presence of 10 μM TF[a]

| | | app rate constant (s^{-1})/10^{-2} | |
	concn of residual GuHCl (M)	k_1	k_2
GFPuv	0.06	5.42 ± 0.15	1.09 ± 0.04
GFPuv + TF	0.06	2.20 ± 0.06	
GFPuv	0.18	3.57 ± 0.07	0.71 ± 0.10
GFPuv + TF	0.18	1.00 ± 0.01	
GFPuv	0.25	2.34 ± 0.04	
GFPuv + TF	0.25	0.80 ± 0.01	
GFPuv	0.50	0.44 ± 0.01	
GFPuv + TF	0.50	0.23 ± 0.01	

[a] The concentration of GFPuv was 0.2 μM. The data shown are the mean $\pm$ the standard error derived from at least 3 separate measurements.

tion of 0.06 M. This suggests high-energy barriers for both the unfolding and refolding reactions (*48*). A number of folding intermediate states have been detected under various denaturing conditions (*11−13*, *49*). Using guanidine as the denaturant, we likewise found that the folding of GFPuv occurs in a stepwise manner and intermediates can be detected under both equilibrium and kinetic folding conditions (Figures 2, 3 and 4; Tables 1 and 2). The formation of the backbone structure of GFPuv is essential but not sufficient to allow the chromophore to attain its native fluorescence, which suggests that a very slow adjustment of the microenvironment around the tripeptide chromophore motif occurs after the backbone has formed.

Trigger factor is a nucleotide-independent molecular chaperone that combines two functions: chaperone activity and catalysis of prolyl isomerization. The binding affinity of TF for folding intermediates is lower than that of other chaperones, and the binding and release of folding intermediates by TF is a highly dynamic process, which may be related to its role in nascent peptide folding (*37*, *50*). TF-assisted GFPuv refolding is quite different from TF-assisted folding of GAPDH (*35*), RCM-La (*50*), bovine carbonic anhydrase II (*36*) or lysozyme (*37*), in that the spontaneous refolding of GFPuv shows very high yields and almost no aggregation occurs during refolding. We therefore investigated how the folding rate constants are affected by different concentrations of TF. As shown in Figure 5 and Table 3, TF accelerates GFPuv folding at low concentrations and retards GFPuv folding at high concentrations. This phenomenon can be explained by competition between the two functions of TF, namely, catalysis and binding.

TF-assisted refolding of guanidine-denatured GFPuv is a complicated process involving a number of steps. The observed rate constant under a given set of conditions will reflect the slowest step under those conditions, which could be tertiary structure adjustment, prolyl isomerization, or formation of the GFPuv backbone. In addition, formation of intermolecular interactions, such as binding of GFPuv folding intermediates by TF, could also influence the rate of folding. In the presence of concentrations of TF lower than 0.4 μM, the rate of folding was increased, indicating that prolyl isomerization was previously limiting. However, proline isomerization can often be coupled to folding (*36*, *50*, *51*). With increasing TF concentration, the rate of folding was reduced as TF apparently binds and traps folding intermediates of GFPuv, as has been observed for other TF
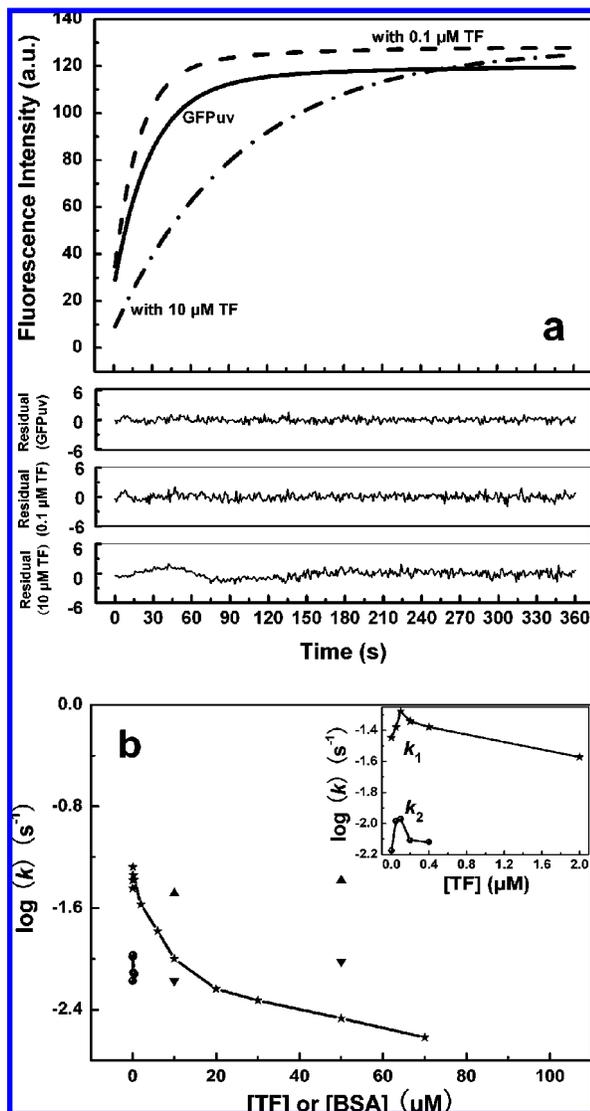
FIGURE 5: (a) Representative refolding curves of GFPuv in the presence or absence of TF monitored by chromophore fluorescence. The refolding of GFPuv was performed by a jump of GuHCl concentration from 6.0 to 0.18 M in Tris buffer at pH 7.5. The refolding of GFPuv alone (—) and with 0.1 μM (— — —) or 10 μM (—•—) TF are shown. The curves of GFPuv refolding alone and in the presence of 0.1 μM TF fit well to double exponentials, whereas the refolding in the presence of 10 μM TF fits well to a single exponential. Plots of the residuals of the fits are shown in the lower panel. (b) Effect of TF concentration on the refolding rate constants of GFPuv, k_1 (★) and k_2 (●), corresponding to formation and adjustment of the chromophore. Effect of BSA, as an inert protein control, on the k_1 (▲) and k_2 (▼) of GFPuv refolding is also shown. The concentrations of GFPuv and residual GuHCl were 0.2 μM and 0.18 M, respectively.

Table 3: The Effect of TF and TF Mutants on the Apparent Rate Constants of GFPuv Refolding Measured by Chromophore Fluorescence[a]

	concn of TF or TF mutants (μM)	app rate constant (s^{-1})/10^{-2}	
		k_1	k_2
GFPuv		5.42 ± 0.15	1.09 ± 0.04
GFPuv + BSA	0.1	5.72 ± 0.13	1.16 ± 0.10
	6	5.72 ± 0.19	1.00 ± 0.01
GFPuv + TF	0.1	7.80 ± 0.15	1.44 ± 0.08
	6	3.70 ± 0.11	0.27 ± 0.01
GFPuv + F233Y-TF	0.1	5.85 ± 0.19	1.04 ± 0.06
	6	2.72 ± 0.10	
GFPuv + NC	0.1	5.20 ± 0.16	1.10 ± 0.06
	6	4.78 ± 0.12	0.61 ± 0.07
GFPuv + NM	0.1	5.32 ± 0.18	0.92 ± 0.07
	6	5.43 ± 0.14	0.91 ± 0.09
GFPuv + MC	0.1	5.42 ± 0.05	0.80 ± 0.08
	6	5.78 ± 0.13	0.81 ± 0.06

[a] The concentrations of GFPuv and residual GuHCl were 0.2 μM and 0.06 M, respectively. The data shown are the mean ± the standard error derived from at least 3 separate measurements.

spontaneously to the correct conformation (central pathway in Scheme 1).

In the presence of TF, the refolding yield of GFPuv does not change with increasing TF concentration. Instead, the refolding rate is affected by the TF concentration. In the presence of low concentrations of TF, the fast regain of Trp57 fluorescence and both fast recovery and slow adjustment phases of the chromophore fluorescence are accelerated, suggesting that those processes are all coupled to proline isomerization, since the presence of equivalent concentrations of BSA or a PPIase activity-impaired mutant of TF (F233Y-TF) did not show the same acceleration in rate. On the other hand, the lack of effect of TF truncation mutants NM and MC, which contain the PPIase domain but are defective in substrate binding (*44*), suggests that the binding (or chaperone) activity of TF may also contribute.

With increasing TF concentration, the rate constants for the rapid burial of Trp57 and for the chromophore fluorescence acquisition and adjustment are all decreased, ultimately leading to observation of a single slow phase (Table 3). These results may be best explained by competition between catalysis and binding by TF. It has been suggested previously that TF assisted protein folding requires repeated binding-and-release cycles between TF and folding intermediates (*35*); the higher the concentration of TF, the greater the chance of recapture of substrate intermediates by TF. This binding effect can lead to arrest of folding (*35, 37, 50*), so that GFPuv folding is no longer limited by proline isomerization. It has been suggested that the monomer−dimer equilibrium of TF is physiology relevant, either because dimeric TF represents a storage form ensuring saturation of ribosomes with TF or because the monomeric and dimeric forms have distinct functions (*31, 32*). The proportion of TF in the dimeric form will increase with the increase in TF concentration in our experiments, and so the very slow release of folding intermediates from the TF complex at high concentrations of TF could be attributed to the tight binding of intermediates by dimeric TF, since the TF dimer can bind with folding-competent intermediates stably *in vitro* (*32*).

In conclusion, TF-assisted folding of GFPuv demonstrates clearly how the two functions of the TF molecule can
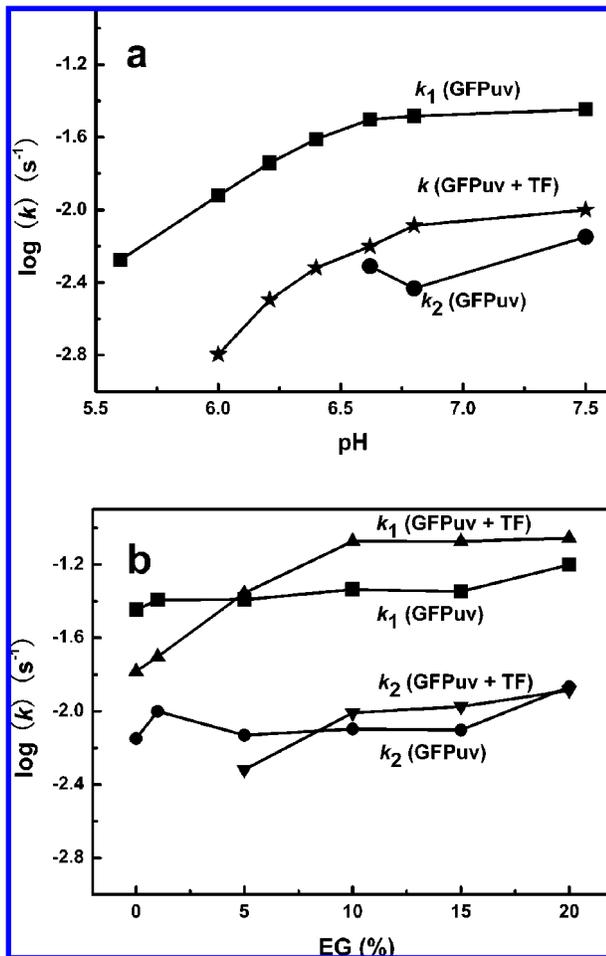
substrates (*35, 37, 50*). In this scenario, the limiting step in folding may involve escape from TF to fold in solution, or could reflect the slow folding of GFPuv while bound to TF.

Scheme 1 presents a hypothetical mechanism for the events that could occur upon dilution of GuHCl denatured GFPuv in the presence of TF. In this model, upon sudden dilution of guanidine denatured GFPuv, rapid collapse of GFPuv occurs to form an intermediate in which Trp57 is buried. The chromophore microenvironment then gradually recovers, and proline isomerization may be coupled to folding. Refolding of GFPuv can reach maximum fluorescence at 508 nm without aggregation, suggesting that GFPuv can fold

FIGURE 6: (a) Effect of pH on the rate constants for spontaneous refolding, k_1 (■) and k_2 (●), and TF assisted refolding (★) of GFPuv. The concentrations of GFPuv and residual GuHCl were 0.2 μM and 0.18 M, respectively. The TF concentration was 10 μM if present. The refolding buffers with different pH values were prepared as described in Methods. (b) Effect of ethylene glycol (EG) concentration on the rate constants for spontaneous refolding, k_1 (■) and k_2 (●), and TF assisted refolding, k_1 (▲) and k_2 (▼), of GFPuv. Refolding was performed in Tris buffer (pH 7.5) containing different concentrations of EG. The concentrations of GFPuv and residual GuHCl were 0.2 μM and 0.18 M, respectively. The TF concentration was 6 μM if present.

Scheme 1: A Simplified Scheme for TF Assisted GFPuv Refolding[a]
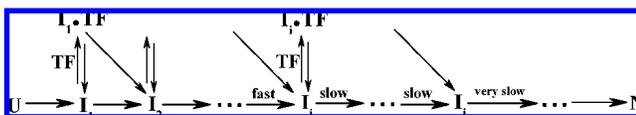
[a] The central left-to-right path illustrates the route of spontaneous folding of GFPuv. U is the guanidine-denatured state. I_1, I_2, $I_i - I_{j-1}$ are all possible folding intermediates that can transiently associate with TF, where their further folding involves proline isomerization. I_j to the last intermediate before the native state represent the intermediates that no longer specifically bind with TF. N represents the native state. In the presence of TF, those intermediate states that can react with TF will give rise to a change in the refolding rates. The extent of the effect on the refolding rate depends on the concentration of TF: TF accelerates proline isomerization at low concentrations and retards GFPuv folding at high concentrations.

combine to modulate folding of a substrate protein: as a PPIase, TF catalyzes proline isomerization and so can accelerate the proline-limited folding of GFPuv; while as a chaperone, TF binds and traps folding intermediates of

GFPuv, which can lead to a retardation in the folding rate at high TF concentrations.

REFERENCES

1. Ward, T. H., and Lippincott-Schwartz, J. (2006) The uses of green fluorescent protein in mammalian cells, *Methods Biochem. Anal. 47*, 305−337.
2. Amoh, Y., Li, L., Katsuoka, K., Bouvet, M., and Hoffman, R. M. (2007) GFP-expressing vascularization of Gelfoam as a rapid *in vivo* assay of angiogenesis stimulators and inhibitors, *Biotechniques 42*, 294, 296, 298.
3. Magliery, T. J., and Regan, L. (2006) Reassembled GFP: detecting protein-protein interactions and protein expression patterns, *Methods Biochem. Anal. 47*, 391−405.
4. Vasiljevic, S., Ren, J., Yao, Y., Dalton, K., Adamson, C. S., and Jones, I. M. (2006) Green fluorescent protein as a reporter of prion protein folding, *Virol. J. 3*, 59−67.
5. Chang, H. C., Kaiser, C. M., Hartl, F. U., and Barral, J. M. (2005) *De novo* folding of GFP fusion proteins: high efficiency in eukaryotes but not in bacteria, *J. Mol. Biol. 353*, 397−409.
6. Lalonde, S., Ehrhardt, D. W., and Frommer, W. B. (2005) Shining light on signaling and metabolic networks by genetically encoded biosensors, *Curr. Opin. Plant Biol. 8*, 574−581.
7. Battistutta, R., Negro, A., and Zanotti, G. (2000) Crystal structure and refolding properties of the mutant F99S/M153T/V163A of the green fluorescent protein, *Proteins 41*, 429−437.
8. Fukuda, H., Arai, M., and Kuwajima, K. (2000) Folding of green fluorescent protein and the cycle3 mutant, *Biochemistry 39*, 12025−12032.
9. Merkel, J. S., and Regan, L. (2000) Modulating protein folding rates *in vivo* and *in vitro* by side-chain interactions between the parallel beta strands of green fluorescent protein, *J. Biol. Chem. 275*, 29200−29206.
10. Iwai, H., Lingel, A., and Pluckthun, A. (2001) Cyclic green fluorescent protein produced *in vivo* using an artificially split PI-PfuI intein from *Pyrococcus furiosus*, *J. Biol. Chem. 276*, 16548−16554.
11. Enoki, S., Saeki, K., Maki, K., and Kuwajima, K. (2004) Acid denaturation and refolding of green fluorescent protein, *Biochemistry 43*, 14238−14248.
12. Enoki, S., Maki, K., Inobe, T., Takahashi, K., Kamagata, K., Oroguchi, T., Nakatani, H., Tomoyori, K., and Kuwajima, K. (2006) The equilibrium unfolding intermediate observed at pH 4 and its relationship with the kinetic folding intermediates in green fluorescent protein, *J. Mol. Biol. 361*, 969−982.
13. Huang, J. R., Craggs, T. D., Christodoulou, J., and Jackson, S. E. (2007) Stable intermediate states and high energy barriers in the unfolding of GFP, *J. Mol. Biol. 370*, 356−371.
14. Pedelacq, J. D., Cabantous, S., Tran, T., Terwilliger, T. C., and Waldo, G. S. (2006) Engineering and characterization of a superfolder green fluorescent protein, *Nat. Biotechnol. 24*, 79−88.
15. Suno, R., Taguchi, H., Masui, R., Odaka, M., and Yoshida, M. (2004) Trigger factor from *Thermus thermophilus* is a Zn^{2+}-dependent chaperone, *J. Biol. Chem. 279*, 6380−6384.
16. Ziętkiewicz, S., Krzewska, J., and Liberek, K. (2004) Successive and synergistic action of the Hsp70 and Hsp100 chaperones in protein disaggregation, *J. Biol. Chem. 279*, 44376−44383.
17. Yoshida, T., Iizuka, R., Itami, K., Yasunaga, T., Sakuraba, H., Ohshima, T., Yohda, M., and Maruyama, T. (2007) Comparative analysis of the protein folding activities of two chaperonin subunits of *Thermococcus* strain KS-1: the effects of beryllium fluoride, *Extremophiles 11*, 225−235.
18. Hesterkamp, T., Hauser, S., Lutcke, H., and Bukau, B. (1996) *Escherichia coli* trigger factor is a prolyl isomerase that associates with nascent polypeptide chains, *Proc. Natl. Acad. Sci. U.S.A. 93*, 4437−4441.
19. Baram, D., Pyetan, E., Sittner, A., uerbach-Nevo, T., Bashan, A., and Yonath, A. (2005) Structure of trigger factor binding domain

in biologically homologous complex with eubacterial ribosome reveals its chaperone action, *Proc. Natl. Acad. Sci. U.S.A. 102*, 12017−12022.

20. Hoffmann, A., Merz, F., Rutkowska, A., Zachmann-Brand, B., Deuerling, E., and Bukau, B. (2006) Trigger factor forms a protective shield for nascent polypeptides at the ribosome, *J. Biol. Chem. 281*, 6539−6545.

21. Stoller, G., Rucknagel, K. P., Nierhaus, K. H., Schmid, F. X., Fischer, G., and Rahfeld, J. U. (1995) A ribosome-associated peptidyl-prolyl *cis/trans* isomerase identified as the trigger factor, *EMBO J. 14*, 4939−4948.

22. Stoller, G., Tradler, T., Rucknagel, K. P., Rahfeld, J.-U., and Fischer, G. (1996) An 11.8 kDa proteolytic fragment of the *E. coli* trigger factor represents the domain carrying the peptidyl-prolyl *cis/trans* isomerase activity, *FEBS Lett. 384*, 117−122.

23. Hesterkamp, T., and Bukau, B. (1996) Identification of the prolyl isomerase domain of *Escherichia coli* trigger factor, *FEBS Lett. 385*, 67−71.

24. Ferbitz, L., Maier, T., Patzelt, H., Bukau, B., Deuerling, E., and Ban, N. (2004) Trigger factor in complex with the ribosome forms a molecular cradle for nascent proteins, *Nature 431*, 590−596.

25. Li, Z. Y., Liu, C. P., Zhu, L. Q., Jing, G. Z., and Zhou, J. M. (2001) The chaperone activity of trigger factor is distinct from its isomerase activity during co-expression with adenylate kinase in *Escherichia coli*, *FEBS Lett. 506*, 108−112.

26. Kramer, G., Patzelt, H., Rauch, T., Kurz, T. A., Vorderwulbecke, S., Bukau, B., and Deuerling, E. (2004) Trigger factor peptidyl-prolyl *cis/trans* isomerase activity is not essential for the folding of cytosolic proteins in *Escherichia coli*, *J. Biol. Chem. 279*, 14165−14170.

27. Genevaux, P., Keppel, F., Schwager, F., Langendijk-Genevaux, P.S., Hartl, F.U., and Georgopoulos, C. (2004) *In vivo* analysis of the overlapping functions of DnaK and trigger factor, *EMBO Rep. 5*, 195−200.

28. Kramer, G., Rutkowska, A., Wegrzyn, R. D., Patzelt, H., Kurz, T. A., Merz, F., Rauch, T., Vorderwulbecke, S., Deuerling, E., and Bukau, B. (2004) Functional dissection of *Escherichia coli* trigger factor: unraveling the function of individual domains, *J. Bacteriol. 186*, 3777−3784.

29. Merz, F., Hoffmann, A., Rutkowska, A., Zachmann-Brand, B., Bukau, B., and Deuerling, E. (2006) The C-terminal domain of *Escherichia coli* trigger factor represents the central module of its chaperone activity, *J. Biol. Chem. 281*, 31963−31971.

30. Kramer, G., Rauch, T., Rist, W., Vorderwulbecke, S., Patzelt, H., Schulze-Specking, A., Ban, N., Deuerling, E., and Bukau, B. (2002) L23 protein functions as a chaperone docking site on the ribosome, *Nature 419*, 171−174.

31. Patzelt, H., Kramer, G., Rauch, T., Schonfeld, H. J., Bukau, B., and Deuerling, E. (2002) Three-state equilibrium of *Escherichia coli* trigger factor, *Biol. Chem. 383*, 1611−1619.

32. Liu, C. P., Perrett, S., and Zhou, J. M. (2005) Dimeric trigger factor stably binds folding-competent intermediates and cooperates with the DnaK-DnaJ-GrpE chaperone system to allow refolding, *J. Biol. Chem. 280*, 13315−13320.

33. Lakshmipathy, S. K., Tomic, S., Kaiser, C. M., Chang, H. C., Genevaux, P., Georgopoulos, C., Barral, J. M., Johnson, A. E., Hartl, F. U., and Etchells, S. A. (2007) Identification of nascent chain interaction sites on trigger factor, *J. Biol. Chem. 282*, 12186−12193.

34. Scholz, C., Stoller, G., Zarnt, T., Fischer, G., and Schmid, F. X. (1997) Cooperation of enzymatic and chaperone functions of trigger factor in the catalysis of protein folding, *EMBO J. 16*, 54−58.

35. Huang, G. C., Li, Z. Y., Zhou, J. M., and Fischer, G. (2000) Assisted folding of D-glyceraldehyde-3-phosphate dehydrogenase by trigger factor, *Protein Sci. 9*, 1254−1261.

36. Liu, C. P., and Zhou, J. M. (2004) Trigger factor-assisted folding of bovine carbonic anhydrase II, *Biochem. Biophys. Res. Commun. 313*, 509−515.

37. Huang, G. C., Chen, J. J., Liu, C. P., and Zhou, J. M. (2002) Chaperone and antichaperone activities of trigger factor, *Eur. J. Biochem. 269*, 4516−4523.

38. Pace, C. N. (1986) Determination and analysis of urea and guanidine hydrochloride denaturation curves, *Methods Enzymol. 131*, 266−280.

39. Gill, S. C., and von Hippel P. H. (1989) Calculation of protein extinction coefficients from amino acid sequence data, *Anal. Biochem. 182*, 319−326.

40. Zeng, L. L., Yu, L., Li, Z. Y., Perrett, S., and Zhou, J. M. (2006) Effect of C-terminal truncation on the molecular chaperone function and dimerization of *Escherichia coli* trigger factor, *Biochimie 88*, 613−619.

41. Ward, W. W., Prentice, H. J., Roth, A. F., Cody, C. W., and Reeves, S. C. (1982) Spectral perturbations of the *Aequorea* green-fluorescent protein, *Photochem. Photobiol. 35*, 803−808.

42. Ellman, G. L. (1959) Tissue sulfhydryl groups, *Arch. Biochem. Biophys. 82*, 70−77.

43. Pace, C. N., and Scholtz, J. M. (1997) Measuring the conformational stability of a protein, in *Protein Structure* (Creighton, T. E., Ed.) 2nd ed., pp 261−298, IRL Press, Oxford.

44. Zarnt, T., Tradler, T., Stoller, G., Scholz, C., Schmid, F. X., and Fischer, G. (1997) Modular structure of the trigger factor required for high activity in protein folding, *J. Mol. Biol. 271*, 827−837.

45. Kneen, M., Farinas, J., Li, Y., and Verkman, A. S. (1998) Green fluorescent protein as a noninvasive intracellular pH indicator, *Biophys. J. 74*, 1591−1599.

46. Elsliger, M. A., Wachter, R. M., Hanson, G. T., Kallio, K., and Remington, S. J. (1999) Structural and spectral response of green fluorescent protein variants to changes in pH, *Biochemistry 38*, 5296−5301.

47. Jackson, S. E. (1998) How do small single-domain proteins fold?, *Fold. Des. 3*, R81−R91.

48. Jackson, S. E., Craggs, T. D., and Huang, J. R. (2006) Understanding the folding of GFP using biophysical techniques, *Expert. Rev. Proteomics 3*, 545−559.

49. Herberhold, H., Marchal, S., Lange, R., Scheyhing, C. H., Vogel, R. F., and Winter, R. (2003) Characterization of the pressure-induced intermediate and unfolded state of red-shifted green fluorescent protein—a static and kinetic FTIR, UV/VIS and fluorescence spectroscopy study, *J. Mol. Biol. 330*, 1153−1164.

50. Maier, R., Scholz, C., and Schmid, F. X. (2001) Dynamic association of trigger factor with protein substrates, *J. Mol. Biol. 314*, 1181−1190.

51. Galani, D., Fersht, A. R., and Perrett, S. (2002) Folding of the yeast prion protein Ure2: kinetic evidence for folding and unfolding intermediates, *J. Mol. Biol. 315*, 213−227.